Electronic Materials Letters, Vol. 4, No. 2 (2008), pp. 71-74

Influence of ZnO Seed Layers on Charge Transport in ZnO Nanorod-based Dye-Sensitized Solar Cells

Jun Hong Noh[1], Sung Hae Lee[2], Sangwook Lee[1], and Hyun Suk Jung[2,*]

[1]School of Materials Science & Engineering, Seoul National University, Seoul 151-742, Korea
[2]School of Advanced Materials Engineering, Kookmin University,
Jeongneung-dong, Seongbuk-gu, Seoul 136-702, Korea

ZnO nanorod array films were deposited on seeded fluorine-doped tin oxide substrates with a chemical bath deposition method, and the dependence of the photovoltaic properties of the films on the annealing temperatures of seed layers was investigated. The energy conversion efficiency of ZnO nanorod-based DSSCs that contained seed layers annealed at 340°C was superior to that of DSSCs consisting of ZnO nanorods on seed layers annealed at 100°C. Electrochemical impedance spectroscopy revealed that the improved energy conversion efficiency is due to the enhancement in the electron transport within the seed layers.

Keywords: ZnO, nanorod, dye-sensitized solar cell, seed, impedance

1. INTRODUCTION

Dye-sensitized solar cells (DSSCs) have attracted interest because of their low cost fabrication and potential application for flexible devices.[1,2] A common photoanode material in DSSCs is 10 μm thick TiO_2 nanoparticle film on transparent conducting oxide (TCO) layers. The popularity of this material is due to its adequate surface area and chemical affinity for dye adsorption as well as its suitable energy band potential for charge transfer with dye and electrolytes. However, numerous grain boundaries between TiO_2 nanoparticles restrict the fast electron transport. As an improvement to electron transport in the anode of DSSCs, ZnO nanorods or nanowires with a high surface area were recently exploited as a photoanode. Each ZnO nanorod or nanowire has single crystals without grain boundaries and the energy band position is close to that of TiO_2; as a result, this type of material is considered suitable for high performance photoanodes.[3,4] However, the best efficiency (η) of ZnO nanorod-based DSSCs is 1.5%, which is inferior to the approximately 11% efficiency level of TiO_2 nanoparticle-based DSSCs.[3]

ZnO nanorod-based DSSCs are still challenging and need to be studied further so that their photovoltaic properties can be improved. For example, suitable electrolyte and dye materials need to be developed, and the fabrication parameters and design of the nanostructure need to be optimized, which is essential for maximizing the energy conversion efficiency. Wu *et al.*[5] recently reported that a mercurochrome ($C_{20}H_8Br_2HgNa_2O$) sensitizer is more suitable than the currently used $Ru(dcbpy)_2(NCS)_2$ (N3) dye for ZnO nanorod-based DSSCs. This finding illustrates the need for extensive studies on ZnO nanorod-based DSSCs.

In our report, the effect of ZnO nanoparticle seed layers on the performance of DSSCs was investigated. The annealing temperature of a seed layer was found to significantly influence the charge transport property of ZnO nanorod-based DSSCs. Electrochemical impedance spectroscopy (EIS) analysis confirmed that the annealing temperature of seed layers is critical for improving the energy conversion efficiency of ZnO nanorod-based DSSCs.

2. EXPERIMENTAL PROCEDURE

ZnO nanoparticles, which are used as seed layers, were prepared by hydrolysis of zinc acetate dehydrate and lithium hydroxide monohydrate. The details are shown elsewhere.[3] The ZnO seed layers were deposited on F:SnO_2 (FTO) TCO substrates by means of spin coating and then annealed at 100°C or 340°C in air for 5 min. The spin coating and an intermediate annealing process were repeated five times, and the resultant thickness of each seed layer was measured with the aid of field emission scanning electron microscopy (FESEM). The ZnO nanorod arrays were grown on FTO substrates seeded with ZnO nanocrystals by means of a chemical bath deposition method in an aqueous solution of zinc nitrate hexahydrate, hexamethylenetetramine, and polyethyleneimine at 95°C. FESEM was used to examine the morphologies of the deposited materials. The crystal struc-

*Corresponding author: hjung@kookmin.ac.kr

ture and morphology of the synthesized ZnO nanorod arrays were investigated with the aid of high-resolution transmission electron microscopy (HRTEM). To fabricate the DSSCs, we used procedure published in our previous report.[6] The curves of photocurrent density (J) and voltage (V), as well as the EIS measurements of ZnO nanorod-based DSSCs, were measured with a potentiostat under AM 1.5 simulated sunlight at 100 mW cm^{-2}. The effective cell area for all the samples was approximately 0.25 cm^2. The DSSCs with the ZnO nanorod arrays, which were grown on seed layers annealed at 100 and 340°C, were designated as 100-ZnO NR DSSC and 340-ZnO NR DSSC, respectively.

3. RESULTS AND DISCUSSION

Figures 1(a) and 1(b) show cross-sectional FESEM images of the prepared ZnO nanorod arrays on ZnO seed layers annealed at 100 and 340°C. The ZnO nanorods, which had a diameter in the range of 30 to 50 nm and a length of approximately 400 nm, were successfully grown on seed layers annealed at 100 and 340°C. Figure 1(c) shows a TEM image of ZnO nanocrystalline seeds, which have a diameter of approximately 10 nm. Although the seed layers were spin-coated five times on an FTO substrate, the thickness of the seed layers varied significantly between samples annealed at 100 and 340°C, as shown in Figs. 1(a) and 1(b). The thickness of the seed layer annealed at 340°C is approximately 90 nm thinner than the 240 nm thick seed layer annealed at 100°C. This difference is related to the difference in the degree of sintering with the annealing temperature. The sintering process, which eliminates pores between particles and promotes densification of bulk or thin films, is responsible for variations in the thickness of the ZnO seed layers annealed at 100 and 340°C. Given that the ZnO nanocrystals have a high surface area and are fairly reactive, the driving force is high enough for the sintering to take place at 340°C. However, the annealing at 100°C is insufficient for the sintering of nanoparticles; as a result, the seed layer annealed at 100°C has a thick porous structure. Although the seed layers annealed at 100 and 340°C both have different nanostructures, the morphology and crystal quality of the ZnO nanorods, which are grown on the seed layers, are almost identical. That is, the aspect ratio (the diameter/length) of the ZnO nanorods is approximately 1/6, and the ZnO nanorods have similar crystal qualities. As illustrated in Fig. 1(d), the HRTEM image and the selected area diffraction pattern of ZnO nanorod array, which was grown on a seed layer annealed at 100°C illustrate that the ZnO nanorods possess a single crystal structure and that their longitudinal axis direction is perpendicular to the ZnO (001) crystal planes.

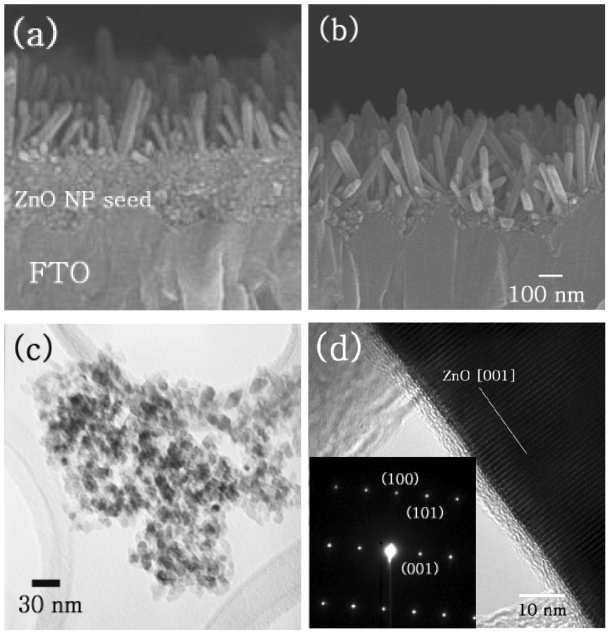

Fig. 1. Cross-sectional SEM images of a ZnO nanorod array in which the seed layer was annealed on an FTO substrate at (a) 100 and (b) 340°C. HRTEM images of (c) ZnO nanoparticles as the seed and (d) a ZnO nanorod. (Inset is a SAD pattern of the ZnO nanorod.)

DSSCs were prepared by using ZnO nanorod arrays on seed layers annealed at 100°C and 340°C. Figure 2 shows

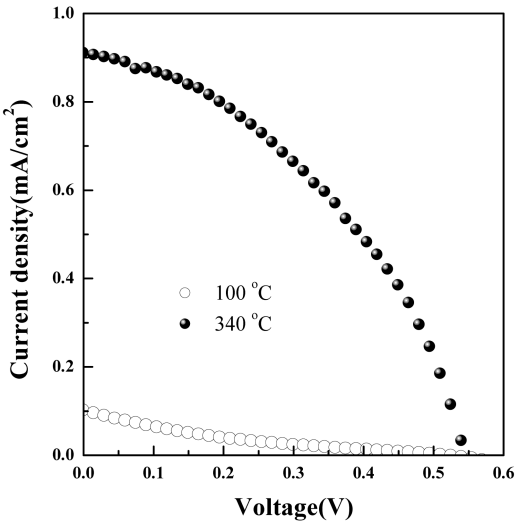

Fig. 2. Photocurrent density vs. voltage curve for DSSCs prepared by using ZnO nanorods on seed layers annealed at 100 and 340°C. Light intensity: 100 mW/cm^2.

Table 1. Performances of DSSCs prepared using ZnO nanorods on 100 and 340°C-annealed seed layers. (efficiency: η, short circuit current density: J_{SC}, open circuit voltage: V_{OC}, and fill factor: *FF*)

DSSC	η (%)	J_{SC} (mA/cm^2)	V_{OC} (V)	*FF* (%)
100-ZnO NR DSSC	0.008	0.1	0.525	15
340-ZnO NR DSSC	0.21	0.9	0.545	41

the photocurrent density (J) and voltage (V) characteristics of the ZnO nanorod-based DSSCs. The performances of both ZnO nanorod DSSCs are summarized in Table 1. The overall efficiency (η) of 0.21% in the 340-ZnO NR DSSC is comparable to that of ZnO nanorod-based DSSCs in previous reports.[7] The value of J_{SC} for the 340-ZnO NR DSSC is 0.9 mA/cm^2, which is remarkably higher than the corresponding value of 0.1 mA/cm^2 for the 100-ZnO NR DSSC. Because the 340 and 100-ZnO NR DSSCs both consist of ZnO nanorod arrays of almost the same dimensions, the difference in the J_{SC} value is not attributed to the amount of dye adsorption on the ZnO nanorod surface. Moreover, the electron transport through the ZnO nanorods does not significantly influence J_{SC} discrepancy because the ZnO nanorod arrays that were grown on seed layers annealed at 100 and 340°C have an almost identical crystal structure. Therefore, the difference in the seed layers annealed at 100 and 340°C is responsible for the significant change in the J_{SC} values of the resultant DSSCs. The facile electron transport properties from anode materials such as TiO_2 and ZnO to TCO reportedly help improve the values of J_{SC} and the fill factor (FF) in DSSCs.[8] In our results, the remarkably enhanced fill factor for the 340-ZnO NR DSSC indicates that the annealing process at 340°C facilitates the charge transport between the ZnO nanoparticles themselves and between the ZnO nanoparticles and the FTO interface. Because the ZnO nanorods have no grain boundaries, the electrical contact between the ZnO nanocrystals is critical in terms of determining the cell performance.

EIS is a useful tool for investigating the electron transport properties in DSSCs. Hoshikawa *et al.*[9] reported that a Nyquist plot of a TiO_2-based DSSC contains ohmic resistance (R_0) and four arcs (ω_1 to ω_4) in a frequency range of 10^{-2} to 10^5 Hz. The existence of electrochemical interfaces generates impedance factors, which are apparently observed as arcs in the Nyquist plot. The characteristic frequency of ω at the top of this arc has a special value defined as $\omega = (RC)^{-1}$ where R is the resistance and C is the capacitance at an electrochemical interface. The arc of ω_1 (10^5 to 10^3 Hz), ω_2 (10^3 to 1 Hz), and ω_3 (1 to 10^{-2} Hz) are associated with the resistance of the electrochemical interface at TCO/TiO_2, TiO_2 nanoparticles/TiO_2 nanoparticles or TiO_2/electrolyte and the resistance of Nerst diffusion in the electrolytes, respectively. In the case of the TiO_2 anode, which is annealed at a low temperature, the arc at ω_2 is mainly associated with the impedance from TiO_2 nanoparticles/TiO_2 nanoparticles. Our ZnO nanorod-based DSSCs also have the three impedance factors of the ZnO seed layer/FTO, ZnO nanoparticles/ZnO nanoparticles or ZnO nanorods/electrolytes, and Nerst diffusion in the electrolytes. Figure 3 shows Nyquist plots for the 100 and 340-ZnO NR DSSCs. A special feature of both Nyquist plots is that the border between the arcs in the high frequency range (ω_1 to ω_3) is vague and that these arcs

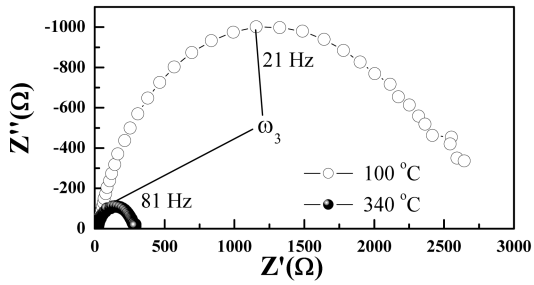

Fig. 3. Nyquist plots for DSSCs prepared by using ZnO nanorods on seed layers annealed at 100 and 340°C. Light intensity: 100 mW/cm^2.

appear as one semicircle. In addition, the semicircle of ω_2 in the 100-ZnO NR DSSC is considerably larger than that in 340-ZnO NR DSSC. According to Hoshikawa *et al.*,[9] a decrease in the calcination temperature induces insufficient sintering of TiO_2 nanoparticles and enlarges the ω_2 semicircle in the TiO_2-based DSSC; this phenomenon is attributed to the large impedance from the presence of numerous grain boundaries between the TiO_2 nanoparticles. In our Nyquist plots, the large semicircle for the 100-ZnO NR DSSC indicates that the low-temperature annealing process of the ZnO seed layers retards the electron transport between the ZnO nanocrystals. In contrast, the tiny semicircle for the 340-ZnO NR DSSC illustrates that the impedance from the ZnO nanocrystal interfaces is significantly reduced, thereby facilitating the charge transport properties. These results demonstrate that the seed annealing process is a critical factor in determining the performance of ZnO nanorod-based DSSCs.

4. CONCLUSIONS

In conclusion, ZnO nanorod arrays were grown on ZnO-seeded FTO substrates by using a chemical bath deposition method, and the annealing temperature of the ZnO seed layers was found to determine the performance of the ZnO nanorod-based DSSCs. EIS confirmed that the significant enhancement in the short circuit current density (J_{SC}), the fill factor (FF), and the overall efficiency (η) of the DSSC containing a ZnO seed layer annealed at 340°C can be ascribed to the facilitated charge transport between the ZnO nanoparticles because of the sufficient sintering of the ZnO nanoparticles. These findings demonstrate that a ZnO nanorod-based DSSC can be highly efficient as a result of the enhanced contact between the ZnO nanocrystals in the seed layer.

ACKNOWLEDGEMENTS

This work was supported by a grant from the Korea Science and Engineering Foundation (KOSEF) of the Korean government (MEST) (R11-2005-048-00000-0, ERC, CMPS). It was also supported by the Seoul R&BD Program and the research program 2007 of Kookmin University in Korea.

REFERENCES

1. B. Oregan and M. Gratzel, *Nature (London)* **353**, 737 (1991).
2. C. Y. Jiang, X. W. Sun, K. W. Tan, G. Q. Lo, A. K. K. Kyaw, and D. L. Kwong, *Appl. Phys. Lett.* **92**, 143101 (2008).
3. M. Law, L. E. Greene, J. C. Johnson, R. Saykally, and P. D. Yang, *Nat. Mater.* **4**, 455 (2005).
4. E. Galoppini, J. Rochford, H. H. Chen, G. Saraf, Y. C. Lu, A. Hagfeldt, and G. Boschloo, *J. Phys. Chem. B* **110**, 16159 (2006).
5. J.-J Wu, G.-R. Chen, H.-H. Yang, C.-H. Ku, and J.-Y. Lai, *Appl. Phys. Lett.* **90**, 213109 (2007).
6. S. Lee, J. Y. Kim, S. H. Youn, M. Park, K. S. Hong, H. S. Jung, J.-K. Lee, and H. Shin, *Langmuir* **23**, 11907 (2007).
7. C.-H. Ku, H.-H. Yang, G.-R. Chen, and J.-J. Wu. *Crys. Growth Des.* **8**, 283 (2007).
8. G. Kron, T. Egerter, J. H. Werner, and U. Rau, *J. Phys. Chem. B* **107**, 3556 (2003).
9. T. Hoshikawa, M. Yamada, R. Kikuchi, and K. Eguchi, *J. Electrochem. Soc.* **152**, E68 (2005).